Electron transport through a quantum dot in the Coulomb blockade regime: Nonequilibrium Green's function based model

Natalya A. Zimbovskaya

Department of Physics and Electronics, University of Puerto Rico-Humacao, CUH Station, Humacao, Puerto Rico 00791, USA; Institute for Functional Nanomaterials, University of Puerto Rico, San Juan, Puerto Rico 00931, USA; and Institute for Nanoelectronics and Computing, School of Electrical and Computer Engineering, Purdue University, 465 NW Avenue, West Lafayette, Indiana 47907, USA

(Received 27 December 2007; revised manuscript received 22 March 2008; published 28 July 2008)

We explore electron transport through a quantum dot coupled to the source and drain charge reservoirs. We trace the transition from the Coulomb blockade regime to Kondo regime in the electron transport through the dot occurring when we gradually strengthen the coupling of the dot to the charge reservoirs. The current-voltage (I-V) characteristics are calculated using the equations of motion approach within the nonequilibrium Green's function formalism beyond the Hartree-Fock approximation. We show that within the Coulomb blockade regime the I-V characteristics for the quantum dot containing a single spin-degenerated level with the energy E_0 include two steps whose locations are determined by the values of E_0 and the energy of Coulomb interaction of electrons in the dot U. The heights of the steps are related as 2:1 which is consistent with the results obtained by means of the transition rate equations.

DOI: 10.1103/PhysRevB.78.035331 PACS number(s): 73.23.Hk, 72.10.Di, 73.63.−b

I. INTRODUCTION

As known, quantum dots host such interesting quantum transport phenomena as Coulomb blockade[1] and Kondo effect.[2,3] Fast development of experimental technique in recent years provides broad opportunities for fabrication of devices including novel active elements such as single molecules, nanowires, and carbon nanotubes, placed in between metallic leads. Such junctions are commonly treated as quantum dots coupled to the macroscopic charge reservoirs which play the parts of source and drain in the electron transport. Current achievements in nanoelectronics make it possible to observe electron transport through realistic junctions varying external parameters (source-drain and gate voltages and temperature) and internal characteristics of the junction, e.g., the coupling strength of the quantum dot to the source and drain reservoirs. As a result, both suppression of the electron transport through the quantum dot at small values of the source-drain voltage (V) arising due to the high charging energy inside the dot (Coulomb blockade) and the increase in the electrical conduction of the junction at $V \approx 0$ due to the Kondo effect were repeatedly observed in experiments on molecular and carbon nanotube junctions.[4–14]

The Coulomb blockade occurs when the quantum dot representing a molecule or a carbon nanotube is weakly coupled to the source and drain which means that the charging energies U are much greater than the contact and temperature induced broadening of the electron levels in the dot. Theoretical studies of the electron transport through a quantum dot within the Coulomb blockade regime mostly employ "master" equations for the transition rates between the states of the dot differing by a single electron.[15–18] It was shown that the current-voltage curves for a dot including a single spin-degenerated level exhibit two steps. The steps correspond to the gradual adding/removing two electrons with the different spin orientations to/from the dot. Assuming the symmetric contacts of the dot with both charge reservoirs, the first step in the current-voltage curve must be two times higher than the second one (see Refs. 18 and 19). This result has a clear physical sense. Obviously, one may put the first electron of an arbitrary spin orientation to the empty level in the dot. However, the spin of the second electron added to the dot is already determined by the spin of the first one. So, there are two ways to add/remove the first electron to/from the empty/filled level in the dot but only one way to add/remove the second one.

While the approach based on the transition rate master equations brings sound results within the Coulomb blockade regime, its generalization to the case of stronger coupled junctions is not justified. More sophisticated methods employing various modifications of the nonequilibrium Green's function (NEGF) formalism are developed to analyze electron transport through quantum dots coupled to the leads.[20] These theoretical techniques were repeatedly employed to calculate the retarded/advanced and lesser Green's functions for the dot. The Green's functions are needed to compute the electron density of states (DOS) on the dot where the Kondo peak could be manifested, as well as the electron current through the junction. A commonly used approach within the NEGF is the equations of motion (EOMs) method which was first proposed to describe quantum dot systems by Meir *et al.*[21] This technique enables us to express the relevant Green's functions in terms of higher-order Green's functions. Writing out EOM for the latter, one arrives at the infinite sequence of the equations successively involving Green's functions of higher orders.

To get expressions for the necessary Green's functions this system of EOM must be truncated. Also, higher-order Green's functions still included in the remaining EOM must be approximated to express them by means of the lower-order Green's functions. In outline, this procedure is well known and commonly used. However, in numerous existing papers important details of the above procedure vary which brings different approximations for the relevant Green's

functions. Accordingly, the results of theoretical studies of the quantum dot response vary.

The NEGF formalism was successfully applied to describe the quantum dot response within the Coulomb blockade regime (weak coupling of the dot to the electron reservoirs) using the expressions for both retarded and lesser Green's functions within the Hartree-Fock approximation.[22,23] The results for the electron transport through the quantum dot obtained in these works give the correct ratio of the subsequent current steps, namely, 2:1, assuming the dot to be symmetrically coupled to the leads. It is a common knowledge that within the Hartree-Fock approximation one cannot catch the Kondo peak. To quantitatively describe this effect one may need to include hybridization up to very high orders in calculation of the lead-dot coupling parameters, and the studies aiming at better theoretical analysis of the Kondo effect started by Meir *et al.*[24] are still in progress (see, e.g., Refs. 20, 25, and 26).

Obviously, the Green's functions suitable to reveal the Kondo peak in the electron DOS on the dot must provide the proper description of the transport through the dot within the Coulomb blockade regime when lead-dot couplings are weak. However, usually NEGF based results beyond the Hartree-Fock approximation, successfully employed to describe the Kondo effect and related phenomena, were not applied to the limiting case of the Coulomb blockade. In those works where such application was carried out, the correct ratio of heights of the subsequent current steps—namely, 2:1—was not obtained. For instance, Muralidharan *et al.*[18] reported the results on NEGF calculations which give equal heights of the two steps on the current-voltage curve within the Coulomb blockade regime, and studies of Galperin *et al.*[20] result in the height ratio of about 1.6:1. So, up to present there exists a discrepancy between NEGF and master equation based results. This discrepancy may not be easily disregarded for its existence makes questionable the general and useful results based on the advanced techniques within the NEGF formalism. Recently, the above disagreement was discussed in Ref. 18.

The purpose of the present work is to clarify the issue and to erase the above inconsistency. We apply equation of motion based approach to NEGF method to get a description of both Coulomb blockade and Kondo regimes in the electron transport through a quantum dot within the same computational procedure for the relevant Green's functions. We show that the assumed approximations give correct ratio of heights of the steps in the current-voltage curves within the Coulomb blockade limit and allow us to get the Kondo peak as well. For simplicity, we omit from consideration dissipative effects, and we concentrate on a nonmagnetic quantum dot coupled to nonferromagnetic leads. Obtained results are valid for an arbitrary value of the Coulomb interaction on the dot, assuming that the latter is stronger than dot-lead coupling. Also, the analysis may be generalized to magnetic systems and to dots containing many levels provided that the charging energy is small compared to the adjacent level separations. We remark that the present analysis is confined with using simplest possible approximations for the necessary Green's functions. Therefore we do not take into account corrections proposed in Ref. 26 to better approximate the Kondo peak.

II. MAIN EQUATIONS

We write the Hamiltonian of the junction including the dot and source and drain reservoirs (leads) as

$$H = H_L + H_R + H_D + H_T. \tag{1}$$

Here, the terms H_β $(\beta=L,R)$ correspond to the left and right leads and describe them within the noninteracting particle approximation,

$$H_\beta = \sum_{r\sigma} \epsilon_{r\beta\sigma} c^+_{r\beta\sigma} c_{r\beta\sigma}, \tag{2}$$

where $\epsilon_{r\beta\sigma}$ are the single-electron energies in the electrode β for the electron states r,σ (the index σ labeling spin-up and spin-down electrons) and $c^+_{r\beta\sigma}, c_{r\beta\sigma}$ denote the creation and annihilation operators for the electrodes. We assume that energy levels $\epsilon_{r\beta\sigma}$ in the electron reservoirs are uniformly spaced over the ranges corresponding to the electron conduction bands for both spin orientations. The spacing between two adjacent levels $\delta\epsilon_{\beta\sigma}$ is supposed to be much smaller than the bandwidth $\Delta_{\beta\sigma}$ $(\delta\epsilon_{\beta\sigma}/\Delta_{\beta\sigma} \sim 10^{-4})$.

The term H_D describes the dot itself. Taking into account the electron-electron interaction, this term has the form

$$H_D = \sum_\sigma E_\sigma c^+_\sigma c_\sigma + U c^+_\uparrow c_\uparrow c^+_\downarrow c_\downarrow, \tag{3}$$

where c^+_σ, c_σ are the creation and annihilation operators for the electrons in the dot, $E_\sigma = E_0$ is the energy of the single dot level, and the energy U characterizes the Coulomb interaction of electrons in the dot. We carry out calculations within the low-temperature regime, so U is supposed to significantly exceed the thermal energy kT. The last term in the Hamiltonian [Eq. (1)] describes the coupling of the reservoirs to the dot,

$$H_T = \sum_{r\beta\sigma} \tau^*_{r\beta\sigma} c^+_{r\beta\sigma} c_\sigma + \text{H.c.}, \tag{4}$$

where $\tau_{r\beta\sigma}$ are the coupling parameters describing the coupling of the r,σ electron states belonging to the electrode β to the quantum dot.

Now, we employ the equations of motion method to compute the retarded Green's function for the dot. Since no spin-flip processes on the dot are taken into account, and we assume the electron transport to be spin conserving, we may separately introduce the Green's functions for each spin channel. The computational procedure is described in the Appendix. We obtain

$$G^{rr}_\sigma(E) = \frac{E - E_0 - \Sigma^\sigma_{02} - U(1 - \langle n_{-\sigma}\rangle)}{(E - E_0 - \Sigma_{0\sigma})(E - E_0 - U - \Sigma^\sigma_{02}) + U\Sigma_{1\sigma}}. \tag{5}$$

Here, $\langle n_{-\sigma}\rangle = \langle c^+_{-\sigma} c_{-\sigma}\rangle$, and self-energy corrections are given by

$$\Sigma_{0\sigma} = \sum_{r\beta} \frac{|\tau_{r\beta\sigma}|^2}{E - \epsilon_{r\beta\sigma} + i\eta}, \tag{6}$$

$$\Sigma_{1\sigma} = \sum_{r\beta} |\tau_{r\beta,-\sigma}|^2 f^{\beta}_{r,-\sigma} \left\{ \frac{1}{E - 2E_0 - U + \epsilon_{r\beta,-\sigma} + i\eta} + \frac{1}{E - \epsilon_{r\beta,-\sigma} + i\eta} \right\}, \tag{7}$$

$$\Sigma_{2\sigma} = \sum_{r\beta} |\tau_{r\beta,-\sigma}|^2 \left\{ \frac{1}{E - 2E_0 - U + \epsilon_{r\beta,-\sigma} + i\eta} + \frac{1}{E - \epsilon_{r\beta,-\sigma} + i\eta} \right\}, \tag{8}$$

$$\Sigma^{\sigma}_{02} = \Sigma_{0\sigma} + \Sigma_{2\sigma}. \tag{9}$$

Here, $f^{\beta}_{r\sigma}$ is the Fermi distribution function for the energy $\epsilon_{r\beta\sigma}$ and the chemical potential μ^{β} and η is a positive infinitesimal parameter. Expression (5) for the Green's function $G^{rr}_{\sigma}(E)$ was first derived by Meir *et al.*[21] Later, the same expression was obtained in Ref. 25 and (assuming that the electron energy levels on the leads are spin degenerate) in the book.[19] It was repeatedly used to qualitatively describe the Kondo peak in the electron DOS (see, e.g., Refs. 24 and 25). As shown in these works, the Kondo peak originates from the last term in the denominator of Eq. (5). At low temperatures the real part of the self-energy term $\Sigma_{1\sigma}$ diverges giving rise to the peak at $\mu^L = \mu^R = E$. Better approximations for the Green's function $G^{rr}_{\sigma}(E)$ such as that derived in the Ref. 26 may give better results for the shape and the height of the Kondo peak. However, the very emergence of the latter is accounted for in Eq. (5).

The occupation numbers $\langle n_{\sigma}\rangle = \langle c^{+}_{\sigma} c_{\sigma}\rangle$ and $\langle n_{-\sigma}\rangle = \langle c^{+}_{-\sigma} c_{-\sigma}\rangle$ may be found solving the integral equations of the form

$$\langle n_{\sigma}\rangle = \frac{1}{2\pi} \int dE\, \mathrm{Im}(G^{<}_{\sigma}), \tag{10}$$

where the lesser Green's function $G^{<}_{\sigma}$ is introduced. The function $G^{<}_{\sigma}$ obeys the Keldysh equation,

$$G^{<}_{\sigma}(E) = G^{rr}_{\sigma}(E) \Sigma^{<}_{\sigma} G^{aa}_{\sigma}(E), \tag{11}$$

where $G^{aa}_{\sigma}(E)$ is the Fourier component of the advanced Green's function. The Fourier transform of the lesser Green's function $G^{<}_{\sigma}$ is related to the Fourier transforms of the retarded and advanced Green's functions of form (5), so the quantities $\langle n_{\sigma}\rangle$ and $\langle n_{-\sigma}\rangle$ appear in the integrands in the right-hand sides of Eq. (10) for both spin directions. In further calculations we use the following expression for $\Sigma^{<}_{\sigma}$:

$$\Sigma^{<}_{\sigma} = i \sum_{\beta} f^{\beta}_{\sigma}(E) \Gamma^{\beta}_{\sigma}. \tag{12}$$

Consequently, we have

$$G^{<}_{\sigma} = i G^{rr}_{\sigma}(E) G^{aa}_{\sigma}(E) [\Gamma^{L}_{\sigma} f^{L}_{\sigma}(E) + \Gamma^{R}_{\sigma} f^{R}_{\sigma}(E)], \tag{13}$$

where $f^{L,R}_{\sigma}(E)$ are the Fermi distribution functions for the left/right reservoirs, and

$$\Gamma^{\beta}_{\sigma} = -2\, \mathrm{Im}(\Sigma^{\beta}_{0\sigma}), \tag{14}$$

where

$$\Sigma^{\beta}_{0\sigma} = \sum_{r} \frac{|\tau_{r\beta\sigma}|^2}{E - \epsilon_{r\beta\sigma} + i\eta}. \tag{15}$$

Employing expression (12) for $\Sigma^{<}_{\sigma}$ we assume that the Coulomb interaction of the electrons on the dot does not affect the coupling of the latter to the leads as well as it occurs within the Hartree-Fock approximation.[22] Such assumption agrees with the way of estimating averages in the process of decoupling of high-order Green's functions which was used to derive Eq. (5). It seems reasonable while the dot coupling to the leads is weaker than the characteristic energy of the Coulomb interactions on the dot. The proper choice of approximation for the lesser Green's function is very important for it directly affects the values of occupation numbers $\langle n_{\pm\sigma}\rangle$ and, consequently, the heights of the peaks in the electron DOS in the Coulomb blockade regime. Also, the relative heights of the steps in the current-voltage characteristics depend on the occupation numbers. The employed form for $G^{<}_{\sigma}(E)$ differs form those used in some previous works (see, e.g., Refs. 20 and 25) where extra terms arising due to the Coulomb interaction on the dot are inserted in the expression for $\Sigma^{<}_{\sigma}$. Certainly, one may expect such terms to appear as corrections to the main approximation (12). However, these terms must become insignificant and negligible in the Coulomb blockade regime when the dot is weakly coupled to the leads. The expression for $\Sigma^{<}_{\sigma}$ reported in Ref. 25 does not satisfy this requirement.

Substituting Eq. (5) into Eq. (13) and inserting the result into Eq. (10) we obtain the system of equations to find the mean occupation numbers of electrons on the dot,

$$\langle n_{\pm\sigma}\rangle = P_{\pm\sigma} + U\langle n_{\mp\sigma}\rangle Q_{\pm\sigma} + U^2 \langle n_{\mp\sigma}\rangle^2 R_{\pm\sigma}. \tag{16}$$

Here,

$$P_{\pm\sigma} = \frac{1}{2\pi} \sum_{\beta} \int \Gamma^{\beta}_{\pm\sigma} f^{\beta}_{\sigma}(E) A_{\pm\sigma} A^{+}_{\pm\sigma} dE, \tag{17}$$

$$Q_{\pm\sigma} = \frac{1}{2\pi} \sum_{\beta} \int \Gamma^{\beta}_{\pm\sigma} f^{\beta}_{\sigma}(E) (A_{\pm\sigma} B^{+}_{\pm\sigma} + A^{+}_{\pm\sigma} B_{\pm\sigma}) dE, \tag{18}$$

$$R_{\pm\sigma} = \frac{1}{2\pi} \sum_{\beta} \int \Gamma^{\beta}_{\pm\sigma} f^{\beta}_{\sigma}(E) B_{\pm\sigma} B^{+}_{\pm\sigma} dE, \tag{19}$$

and the expressions for A_{σ} and B_{σ} are obtained using the Green's function [Eq. (5)], namely,

$$A_\sigma = \frac{E - E_0 - U - \Sigma_{02}^\sigma}{(E - E_0 - \Sigma_{0\sigma})(E - E_0 - U - \Sigma_{02}^\sigma) + U\Sigma_{1\sigma}},$$

$$B_\sigma = \frac{1}{(E - E_0 - \Sigma_{0\sigma})(E - E_0 - U - \Sigma_{02}^\sigma) + U\Sigma_{1\sigma}}. \quad (20)$$

When considering a nonmagnetic system, the energy levels in the source and drain (and in the quantum dot as well) are spin degenerated, so $A_\sigma = A_{-\sigma}, B_\sigma = B_{-\sigma}$. Correspondingly the occupation numbers for both spin orientations coincide with each other. In this case $\langle n_\sigma \rangle = \langle n_{-\sigma} \rangle$ are described with the equation

$$\langle n_\sigma \rangle = \frac{1 - UQ - \sqrt{(1 - UQ)^2 - 4U^2RP}}{2U^2R}. \quad (21)$$

When the electron correlations on the quantum dot are weak ($U \to 0$), the result [Eq. (21)] is reduced to $\langle n_\sigma \rangle = P_\sigma$.

Equation (21) is an important result for it gives an explicit analytical expression for the level populations, so we do not need a time-consuming self-consistent iterative procedure to find the occupation numbers.[27] Now, we write the expression for the electric current I flowing through the junction when we apply the voltage V across the latter. This expression was derived by Jauho and co-workers (see Refs. 28 and 29), and it has the form

$$I = \frac{ie}{2\hbar} \sum_\sigma \int \frac{dE}{2\pi} [(\Gamma_\sigma^L f_\sigma^L - \Gamma_\sigma^R f_\sigma^R)(G_\sigma^{rr} - G_\sigma^{aa}) + (\Gamma_\sigma^L - \Gamma_\sigma^R) G_\sigma^<]. \quad (22)$$

Also, we could employ the equivalent expression,

$$I = \frac{ie}{2\hbar} \sum_\sigma \int \frac{dE}{2\pi} [(\Gamma_\sigma^L f_\sigma^L - \Gamma_\sigma^R f_\sigma^R)(G_\sigma^{rr} - G_\sigma^{aa}) - i(\Gamma_\sigma^L f_\sigma^L + \Gamma_\sigma^R f_\sigma^R) G_\sigma^{rr} G_\sigma^{aa} (\Gamma_\sigma^L - \Gamma_\sigma^R)]. \quad (23)$$

Further, we assume the symmetrical voltage division, $\mu_{L,R} = E_F \pm \frac{1}{2} eV$, and we set $E_F = 0$. Also, in further calculations we introduce a gate potential V_g, so that

$$E_0(V_g) = E_0(V_g = 0) + eV_g. \quad (24)$$

The application of the gate voltage shifts the energy level in the dot, so the energies E_0 and $E_0 + U$ become asymmetrically arranged with respect to $E = E_F$. This asymmetry is necessary to obtain two steps in the I-V curve assuming the symmetric voltage division. Otherwise, the contributions to the current from the vicinities of $E = E_0$ and $E = E_0 + U$ become superposed, and only one step emerges.

III. DISCUSSION

To simplify further calculations we assume all coupling strengths to take on the same value, namely, $\tau_{r\beta\sigma} = \tau$. Now, we calculate the current through the junction in the limit of the weak coupling of the dot to the reservoirs ($\tau \ll U$). To carry out the calculations we need to know the nonequilibrium occupation numbers and we compute them using Eq. (21). The occupation numbers are sensitive to the value of the applied voltage at small voltages as shown in Fig. 1. At low values of the bias voltage ($V < 0.4$ V) the assumed dot energy level ($E_0 = -0.2$ eV) is situated below the chemical potentials for both leads. Therefore the dot is able to receive an electron but unable to transfer it to another lead. Accordingly, the average occupation number is close to unity and the electric current through the junction takes on values close to zero (see Fig. 2). At $V = 0.4$ V the dot energy E_0 crosses the chemical potential μ^R, and the dot becomes active in electronic transport. Now, the electron which arrives at the dot from one reservoir may leave it for another reservoir. This results in a pronounced decrease in the average occupation on the dot accompanied by an increase in the current. One more change in both average electron occupation on the

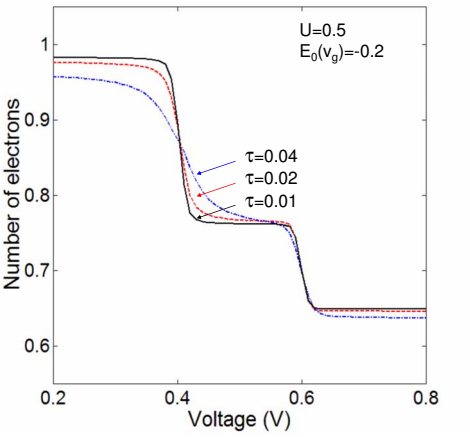

FIG. 1. (Color online) Average occupation numbers in the quantum dot as a function of the voltage applied across the junction. The curves are plotted assuming $U = 0.5$ eV, $kT = 0.000\,26$ eV, $E_0(V_g) = -0.2$ eV, and $\tau = 0.01$ eV (solid line), 0.02 eV (dashed-dotted line), and 0.04 eV (dashed line).

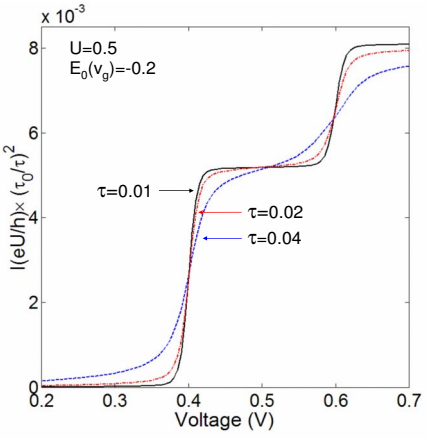

FIG. 2. (Color online) Current through a junction within the Coulomb blockade regime. The curves are plotted assuming $U = 0.5$ eV, $kT = 0.000\,26$ eV, $E_0(V_g) = -0.2$ eV, $\tau_0 = 0.04$ eV, and $\tau = 0.01$ eV (solid line), 0.02 eV (dashed-dotted line), and 0.04 eV (dashed line). The factor τ_0^2/τ^2 is introduced to bring all I-V curves to the same scale. The ratio of heights of the two steps revealed in the curves equals 2:1.

dot and the current through the junction occurs at $V=0.6$ V when the energy $E_0+U(U=0.5$ eV) crosses μ^R. At higher voltage all curves presented in Figs. 1 and 2 level off. The current reaches its maximum value and the average number of electrons in the dot reaches its minimum. The minimum occupation number is noticeably less than 1 but its value is nonzero for electrons unceasingly travel through the junction.

The current-voltage curves in Fig. 2 show typical Coulomb blockade features, namely, two steps whose heights are related as 2:1. So, we see that the results concerning the electron transport through a quantum dot obtained employing the transition rate equations may be quantitatively reproduced within the NEGF formalism when the retarded and lesser Green's functions are approximated by Eqs. (5) and (13), and the explicit expression (21) for the occupation numbers is used. Therefore, the disagreement discussed in the beginning of the present work may be successfully erased, and the consistency between the NEGF formalism and the transition rate equations in the description of the Coulomb blockade regime could be restored beyond the Hartree-Fock approximation.

It is worthwhile to remark that particular values of the average occupation numbers on the dot are very responsive to the gate voltage value V_g (the latter determines how the dot energy level is situated with respect to the Fermi levels of the leads in the absence of the voltage applied across them) and to the Coulomb interaction energy U. Therefore, different values chosen for V_g and U lead to different average occupation numbers. However, under various assumptions for the V_g and U values, one quantity does not vary provided the symmetric coupling of the dot to the leads. This quantity is the relative height of the subsequent steps in the average occupation numbers of the electrons in the dot which are revealed as the voltage across the leads increases. As shown in Fig. 1 this ratio is 2:1, exactly the same as for the subsequent current steps in the I-V curves in Fig. 2. Moreover it is this ratio which ensures the correct shape of I-V curves. For instance, comparing Fig. 1 with the corresponding result reported on the work,[22] one may see that the values of the occupation numbers given in Ref. 22 considerably differ from those obtained in the present work. Nevertheless, the ratio of the subsequent step heights in the occupation numbers versus voltage curves is 2:1, and this provides for the same ratio of heights of the subsequent current steps.

Also, Eqs. (5), (13), and (19) could be applied to analyze the Kondo effect which is manifested at stronger-coupling strengths of the dot to the charge reservoirs. The electron DOS in the dot is given as

$$D(E) = -2\sum_{\sigma} \mathrm{Im}[G^{rr}_{\sigma}(E)]. \tag{25}$$

Using $G^{rr}_{\sigma}(E)$ in form (5) we may compute the electron DOS. The results are presented in Fig. 3 where the equilibrium DOS is shown for three values of the coupling strength τ. For a sufficiently strong coupling of the dot to the source and drain reservoirs ($\tau=0.2$ eV) the sharp Kondo peak appears at $E=0$, and the peaks at $E=E_0$ and $E=E_0+U$ are damped. At weaker-coupling strength ($\tau=0.1$ and 0.07 eV) the

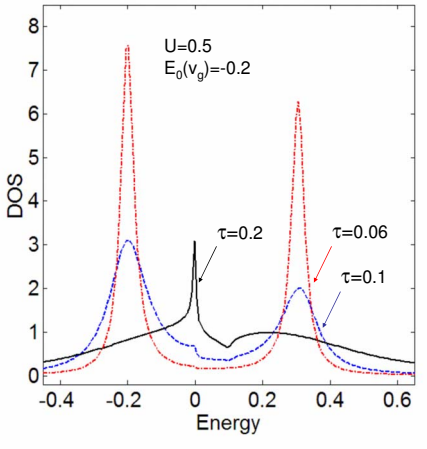

FIG. 3. (Color online) The equilibrium ($V=0$) electron density of states in the quantum dot. The curves are plotted for $\tau=0.2$ eV (solid line), 0.1 eV (dashed line), and 0.06 eV (dashed-dotted line). The remaining parameters are the same as those in Fig. 1.

Kondo peak is reduced to a tiny feature but the maxima at $E=E_0$ and $E=E_0+U$ which determine the conductance within the Coulomb blockade regime emerge. The weaker the coupling is the higher these peaks become.

The heights of the peaks differ. Technically, this distinction originates from the fact that the value of $\langle n_{-\sigma}\rangle$ in the expression for the retarded Green's function [Eq. (5)] differs from 0.5. As shown in the book,[19] assuming $\langle n_{-\sigma}\rangle=\langle n_{\sigma}\rangle=0.5$ one would get the Coulomb blockade peaks of equal height but such assumption leads to the wrong result for the current. Namely, one would obtain two steps of equal height on the current-voltage curves. The physical reason of this difference in the peak heights is the same as for the difference in heights of the steps on the current-voltage characteristics within the Coulomb blockade regime. The latter was discussed in Sec. I. When the voltage is applied across the junction the Kondo peak splits in two maxima whose heights are significantly smaller than the height of the original equilibrium Kondo peak and the greater the voltage is the lower these maxima become. This is shown in Fig. 4. So, the present formalism sufficiently reproduces the results of earlier works concerning the Kondo effect (see, e.g., Refs. 24 and 25).

Finally, in the present work we theoretically analyzed the electron transport through a single-quantum dot coupled to the source and drain charge reservoirs. The analysis was based on the NEGF formalism. Expression (5) for the retarded Green's function was obtained using the equations of motion method and agrees with the results of the previous works.[21,24,25] The lesser Green's function was found from the Keldysh equation using the factor $\Sigma^{<}_{\sigma}$ in form (12). This means that $\Sigma^{<}_{\sigma}$ is supposed to be unchanged due to the Coulomb interactions on the quantum dot, as it is proved to be within the Hartree-Fock approximation. We believe the proposed approximation to be appropriate at moderate and/or weak coupling of the dot to the leads when the coupling strengths are smaller than the characteristic Coulomb energy on the dot. We derived an explicit expression for the occupation numbers of electrons in the dot [Eq. (21)] which en-

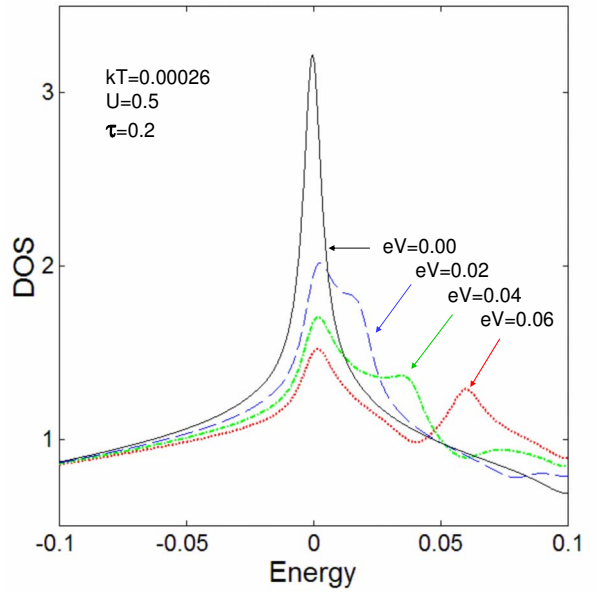

FIG. 4. (Color online) Splitting of the Kondo peak in the electron density of states with increasing bias. The curves are plotted for eV=0 (solid line); 0.02 eV (dashed line), 0.04 eV (dashed-dotted line), and 0.06 eV (dotted line). The coupling strength τ =0.2 eV. The remaining parameters are taken as in Figs. 1 and 2.

ables us to compute them avoiding the long iterative procedure. The employed formalism gives correct results in the Coulomb blockade regime corroborating the results following from the transition rate (master) equations. Our approach is able to quantitatively reproduce the relative heights (2:1) of the steps in the current-voltage curves and to qualitatively describe the Kondo peak using the same expressions for the relevant Green's functions. To the best of our knowledge this was never achieved so far.

Also, we remark that the present work addresses a general problem arising within the NEGF based computations. To quantitatively describe fine features of Kondo effect and related phenomena one needs to include hybridization up to very high orders in calculations of the relevant Green's functions. Carrying out these cumbersome calculations where numerous approximations are inserted, it is easy to make a mistake and difficult to discover one, especially in the absence of obvious small parameters. Probably, such a mistake would not affect the very existence of the Kondo peak but it could distort its fine features. In the present work we propose a method which could help us to verify the resulting expressions for the Green's functions. We start from the clear point, namely, that the Green's functions suitable to describe the Kondo effect are suitable to describe the Coulomb blockade transport as well. Therefore, one may verify obtained results by going to the Coulomb blockade limit. If it occurs that particular Green's functions fail to provide the correct form of the *I-V* curves within this limit, then one must conclude that there is some error in the adopted approximations for the Green's functions.

It is shown that calculational scheme employed in the present work which uses a very simple approximation for $G_\sigma^<$ brings quantitatively correct results for the electron transport through a quantum dot within the Coulomb blockade regime, whereas advanced self-consistent calculations carried out in the recent paper[20] do not. This gives grounds to conjecture that it is not necessary (and, perhaps, it is not always correct) to use the same number of iterations in seeking approximations for retarded/advanced and the lesser Green's functions within EOM method. Also, we remark that validity of the Green's functions used in studies of the Kondo effect may be verified by applying them to calculate electron transport within the Coulomb blockade regime. The results could be generalized to include more realistic case of a dot including many-electron levels, assuming that level separations are much greater than the Coulomb energy U, so one may neglect Coulomb interactions of electrons belonging to different levels.

ACKNOWLEDGMENTS

The author thanks S. Datta for helpful discussions and G. M. Zimbovsky for help with the paper. This work was supported by DoD under Grant No. W911NF-06-1-0519 and NSF under Grant No. DMR-PREM 0353730.

APPENDIX

Here, we explain how expression (5) for the Green's function for the dot is derived. We introduce the following notation for a general retarded Green's function Fourier component:

$$\langle\langle A,B\rangle\rangle \equiv -i\int_0^\infty \langle\{A(t);B\}\rangle e^{i(E+i\eta)t}dt, \tag{A1}$$

where A,B are operators, curly brackets denote the anticommutator, and $\langle\cdots\rangle$ stands for the average. For Hamiltonian (1) the equation of motion for the retarded Green's function for the dot $G_\sigma^{rr}(E)\equiv\langle\langle c_\sigma;c_\sigma^+\rangle\rangle$ reads

$$(E-E_0+i\eta)\langle\langle c_\sigma;c_\sigma^+\rangle\rangle = 1+\sum_{r,\beta}\tau_{r\beta,\sigma}\langle\langle c_{r\beta\sigma};c_\sigma^+\rangle\rangle + U\langle\langle n_{-\sigma}c_\sigma;c_\sigma^+\rangle\rangle. \tag{A2}$$

Here, $n_{-\sigma}\equiv c_{-\sigma}^+c_{-\sigma}$, and the Green's function $\langle\langle c_{r\beta\sigma};c_\sigma^+\rangle\rangle$ obeys the equation

$$(E-\epsilon_{r\beta\sigma}+i\eta)\langle\langle c_{r\beta\sigma};c_\sigma^+\rangle\rangle = \tau_{r\beta\sigma}^*\langle\langle c_\sigma;c_\sigma^+\rangle\rangle. \tag{A3}$$

Substituting the expression for $\langle\langle c_{r\beta\sigma};c_\sigma^+\rangle\rangle$ determined by Eqs. (A3) into Eq. (A2) we get

$$(E-E_0-\Sigma_{0\sigma})\langle\langle c_\sigma;c_\sigma^+\rangle\rangle = 1+U\langle\langle n_{-\sigma}c_\sigma;c_\sigma^+\rangle\rangle, \tag{A4}$$

where the self-energy part $\Sigma_{0\sigma}$ is given by Eq. (6). The equation of motion for the four-operator function $\langle\langle n_{-\sigma}c_\sigma;c_\sigma^+\rangle\rangle$ includes higher order Green's functions. Omitting them, we write out

$$(E-E_0-U+i\eta)\langle\langle n_{-\sigma}c_\sigma;c_\sigma^+\rangle\rangle = \langle n_{-\sigma}\rangle + \sum_{r,\beta}(\tau_{r\beta\sigma}\langle\langle c_{r\beta\sigma}n_{-\sigma};c_\sigma^+\rangle\rangle + \tau_{r\beta;-\sigma}\langle\langle c_{-\sigma}^+c_{r\beta;-\sigma}c_\sigma;c_\sigma^+\rangle\rangle - \tau_{r\beta;-\sigma}^*\langle\langle c_{r\beta;-\sigma}c_{-\sigma}c_\sigma;c_\sigma^+\rangle\rangle). \tag{A5}$$

To proceed we must write equations for the Green's functions inserted in the right side of Eq. (A5). We get

$$(E-\epsilon_{r\beta\sigma}+i\eta)\langle\langle c_{r\beta\sigma}n_{-\sigma};c_\sigma^+\rangle\rangle = \tau_{r\beta\sigma}^*\langle\langle n_{-\sigma}c_\sigma;c_\sigma^+\rangle\rangle + \sum_{r'\beta}(\tau_{r'\beta;-\sigma}\langle\langle c_{r\beta\sigma}c_{-\sigma}^+c_{r'\beta;-\sigma};c_\sigma^+\rangle\rangle - \tau_{r'\beta;-\sigma}^*\langle\langle c_{r'\beta-\sigma}c_{-\sigma}c_{r\beta;\sigma};c_\sigma^+\rangle\rangle), \tag{A6}$$

$$(E-\epsilon_{r\beta;-\sigma}+i\eta)\langle\langle c_{-\sigma}^+c_{r\beta;-\sigma}c_\sigma;c_\sigma^+\rangle\rangle = \tau_{r\beta;-\sigma}^*\langle\langle n_{-\sigma}c_\sigma;c_\sigma^+\rangle\rangle - \sum_{r'\beta}(\tau_{r'\beta-\sigma}\langle\langle c_{r'\beta;-\sigma}^+c_{r\beta;-\sigma}c_\sigma;c_\sigma^+\rangle\rangle + \tau_{r'\beta\sigma}\langle\langle c_{-\sigma}^+c_{r\beta;-\sigma}c_{r'\beta\sigma};c_\sigma^+\rangle\rangle), \tag{A7}$$

$$(E-2E_0-U+\epsilon_{r\beta;-\sigma}+i\eta)\langle\langle c_{r\beta;-\sigma}^+c_{-\sigma}c_\sigma;c_\sigma^+\rangle\rangle = -\tau_{r\beta;-\sigma}\langle\langle n_{-\sigma}c_\sigma;c_\sigma^+\rangle\rangle + \sum_{r'\beta}(\tau_{r'\beta\sigma}\langle\langle c_{r'\beta;-\sigma}^+c_{-\sigma}c_{r\beta\sigma};c_\sigma^+\rangle\rangle - \tau_{r'\beta;-\sigma}\langle\langle c_{r\beta;-\sigma}^+c_\sigma c_{r'\beta;-\sigma};c_\sigma^+\rangle\rangle). \tag{A8}$$

Writing out Eqs. (A6)–(A8) we neglected averages like $\langle c_\sigma^+c_{r\beta\sigma}\rangle$ including a creation/annihilation operator for the dot combined with the annihilation/creation operator for the source/drain reservoir. Such averages are omitted in further calculations as well. Now, we decouple four-operator Green's functions included in the sums over r' in the equations following the scheme,[26]

$$\langle\langle A^+BC;D^+\rangle\rangle \approx \langle A^+B\rangle\langle\langle C;D^+\rangle\rangle - \langle A^+C\rangle\langle\langle B;D^+\rangle\rangle. \tag{A9}$$

Also, we use the approximation

$$\langle c_{r\beta\sigma}^+c_{r'\beta\sigma}\rangle = \langle c_{r'\beta\sigma}c_{r\beta\sigma}^+\rangle = \delta_{rr'}f_{r\sigma}^\beta, \tag{A10}$$

where $f_{r\sigma}^\beta$ is the Fermi distribution function corresponding to the energy $\epsilon_{r\beta\sigma}$. As a result, the Green's functions included in the right-hand side of Eq. (A5) get expressed in terms of the Green's functions $\langle\langle n_{-\sigma}c_\sigma;c_\sigma^+\rangle\rangle$ and $\langle\langle c_\sigma;c_\sigma^+\rangle\rangle$. Substituting these expressions into Eq. (A5) we obtain

$$\langle\langle n_{-\sigma}c_\sigma;c_\sigma^+\rangle\rangle = \frac{\langle n_{-\sigma}\rangle + \Sigma_{1\sigma}\langle\langle c_\sigma;c_\sigma^+\rangle\rangle}{E-E_0-U-\Sigma_{02}^\sigma}. \tag{A11}$$

Here, self-energy parts $\Sigma_{1\sigma},\Sigma_{2\sigma},\Sigma_{02}^\sigma$ are given by

$$\Sigma_{1\sigma} = \sum_{r\beta}|\tau_{r\beta,-\sigma}|^2 f_{r,-\sigma}^\beta\left\{\frac{1}{E-2E_0-U+\epsilon_{r\beta,-\sigma}+i\eta}+\frac{1}{E-\epsilon_{r\beta,-\sigma}+i\eta}\right\}, \tag{A12}$$

$$\Sigma_{2\sigma} = \sum_{r\beta}|\tau_{r\beta,-\sigma}|^2\left\{\frac{1}{E-2E_0-U+\epsilon_{r\beta,-\sigma}+i\eta}+\frac{1}{E-\epsilon_{r\beta,-\sigma}+i\eta}\right\}, \tag{A13}$$

$$\Sigma_{02}^\sigma = \Sigma_{0\sigma}+\Sigma_{2\sigma}. \tag{A14}$$

To arrive at the resulting expression for the dot Green's function $G_\sigma^{rr}\equiv\langle\langle c_\sigma;c_\sigma^+\rangle\rangle$ we substitute Eq. (A11) into Eq. (A4). We have

$$G_\sigma^{rr}(E) = \frac{E-E_0-\Sigma_{02}^\sigma-U(1-\langle n_{-\sigma}\rangle)}{(E-E_0-\Sigma_{0\sigma})(E-E_0-U-\Sigma_{02}^\sigma)+U\Sigma_{1\sigma}}. \tag{A15}$$

[1] M. A. Kastner, Rev. Mod. Phys. **64**, 849 (1992).
[2] L. I. Glazman and M. E. Raikh, JETP Lett. **47**, 452 (1988).
[3] T. K. Ng and P. A. Lee, Phys. Rev. Lett. **61**, 1768 (1988).
[4] J. Park, A. N. Pasupathy, J. I. Goldsmith, C. Chang, Y. Yaish, J. R. Petta, M. Rinkovski, J. P. Sethna, H. D. Abruna, P. I. McEuen, and D. C. Ralph, Nature (London) **417**, 722 (2002).
[5] W. Liang, M. P. Shores, M. Bockrath, J. R. Long, and H. Park, Nature (London) **417**, 725 (2002).
[6] N. B. Zhitenev, H. Meng, and Z. Bao, Phys. Rev. Lett. **88**, 226801 (2002).
[7] J. Reichert, H. B. Weber, M. Mayor, and H. v. Lohneysen, Appl. Phys. Lett. **82**, 4137 (2003).
[8] L. H. Yu and D. l. Natelson, Nano Lett. **4**, 79 (2004).
[9] L. H. Yu, Z. K. Keane, J. W. Ciszek, L. Cheng, M. P. Stewart, J. M. Tour, and D. Natelson, Phys. Rev. Lett. **93**, 266802 (2004).
[10] D. Porath and O. Millo, J. Appl. Phys. **81**, 2241 (1997).
[11] M. Dorogi, J. Gomez, R. Osifchin, R. P. Andres, and R. Reifenberger, Phys. Rev. B **52**, 9071 (1995).
[12] Y. O. Feng, R. Q. Zhang, and S. T. Lee, J. Appl. Phys. **95**, 5729 (2004).
[13] B. I. Leroy, S. G. Lemay, J. Kong, and C. Dekker, Nature (London) **432**, 371 (2004).
[14] K. Grove-Rasmussen, H. I. Jorgensen, and P. E. Lindelof, Physica E (Amsterdam) **40**, 92 (2007).
[15] D. V. Averin and K. K. Likharev, J. Low Temp. Phys. **62**, 345 (1986).

[16] D. V. Averin, A. N. Korotkov, and K. K. Likharev, Phys. Rev. B **44**, 6199 (1991).
[17] S. A. Gurvitz, D. Mozyrsky, and G. P. Berman, Phys. Rev. B **72**, 205341 (2005).
[18] B. Muralidharan, A. W. Ghosh, and S. Datta, Phys. Rev. B **73**, 155410 (2006).
[19] S. Datta, *Quantum Transport: Atom to Transistor* (Cambridge University Press, Cambridge, England, 2005).
[20] See, M. Galperin, A. Nitzan, and M. A. Ratner, Phys. Rev. B **76**, 035301 (2007), and references therein.
[21] Y. Meir, N. S. Wingreen, and P. A. Lee, Phys. Rev. Lett. **66**, 3048 (1991).
[22] R. Świrkowicz, J. Barnaś, and M. Wilczyński, J. Phys.: Condens. Matter **14**, 2011 (2002).
[23] P. Pals and A. MacKinnon, J. Phys.: Condens. Matter **8**, 5401 (1996).
[24] Y. Meir, N. S. Wingreen, and P. A. Lee, Phys. Rev. Lett. **70**, 2601 (1993).
[25] R. Świrkowicz, J. Barnaś, and M. Wilczyński, Phys. Rev. B **68**, 195318 (2003).
[26] V. Kashcheyevs, A. Aharony, and O. Entin-Wohlman, Phys. Rev. B **73**, 125338 (2006).
[27] A similar way of the occupation number calculations was recently proposed by Galperin *et al.* (Ref. 20).
[28] A.-P. Jauho, N. S. Wingreen, and Y. Meir, Phys. Rev. B **50**, 5528 (1994).
[29] H. Hang and A.-P. Jauho, *Quantum Kinetics in Transport and Optics in Semiconductors* (Springer, Berlin, 1996).